RESEARCH ARTICLE

Mathematical Study of Generalized Chemically Reactive NonNewtonain (Eyring-Powell) Material Capturing Varying Thermal Aspect Developing Cattaneo-Christov Concept

Muhammad Zubair[1,*], **Faryal Younis**[2], **Sami Ullah Khan**[3], **Muhammad Waqas**[2] and **Muhammad Zulfiqar**[4]

[1] School of Qilu Transportation, Shandong University, Jinan 250061, China
[2] NUTECH School of Applied Sciences and Humanities, National University of Technology, Islamabad 44000, Pakistan
[3] Department of Mathematics, Namal University, Mainwali 42250, Pakistan
[4] Department of Mathematics, Daanish School Boys Harnooli Mainwali, Punjab 42020, Pakistan

Abstract

This study investigates the effects of a nonlinear stretched surface in a two-dimensional Modified Eyring-Powell liquid due to a double stratified chemical reactive flow of non-Fourier heat flux. We study the flux model which is the generalized form of Fourier's classical expression with thermal relaxation time. The temperature-dependent thermal conductivity is taken into consideration and the stretched surface's thickness is variable. The similarity transformation approach is used to convert the governing system of PDEs into a collection of connected nonlinear ordinary differential systems. The resulting problems are tackled via the application of homotopy analysis approach. Skin friction coefficient, sherwood number, temperature, concentration, and non-dimensional velocity are all visually presented and thoroughly examined.

Keywords: variable sheet thickness, non-linear stretching sheet, non-Fourier heat flux, modified eyring powell liquid, variable thermal conductivity.

1 Introduction

The analysis of extended flows involving chemical reactions is crucial in many branches of research and engineering. The effects of heat and mass transfer in flow cannot be disregarded, especially when building equipment for food processing, freezing crops, producing and dispersing fog, and chemical processing. Furthermore, a wide range of industrial and engineering applications, including metallurgy, combustion systems, solar collectors, chemical engineering, and nuclear reactor safety, rely

Submitted: 05 September 2025
Accepted: 29 September 2025
Published: 27 November 2025

Vol. 1, **No.** 2, 2025.
10.62762/IJTSSE.2025.438295

***Corresponding author:**
✉ Muhammad Zubair
mzubair@sdu.edu.cn

Citation
Zubair, M., Younis, F., Khan, S. U., Waqas, M., & Zulfiqar, M. (2025). Mathematical Study of Generalized Chemically Reactive NonNewtonain (Eyring-Powell) Material Capturing Varying Thermal Aspect Developing Cattaneo-Christov Concept. *International Journal of Thermo-Fluid Systems and Sustainable Energy*, 1(2), 75–82.

on the efficiency of this kind of flow. Chemical reactions' impact was a common feature in study reports written by researchers. When a viscous liquid flows through a permeable channel, for instance, Srinivas studies the chemically reactive flow of the liquid [1]. Zhang et al. [2] examines how heat radiation and chemical reactions affect nanofluid flow through porous material that is saturating it. When chemical processes and transpiration were present, Mabood et al. [3] investigated the MHD flow of a viscous liquid. Casson liquid's chemically reactive flow towards a vertical cone is studied by Mythili and Sivaraj [4]. For a chemically reactive two-phase magneto nanomaterial, Eid [5] proposes an exponentially stretched surface analysis. Thermophoresis, nonlinear thermal radiation, and chemically reactive bioconvective flow of magneto nanomaterial towards the upper horizontal surface of a rotating paraboloid were investigated by Makinde and Animasaun [6].

Numerous technical and industrial processes involve the transport of heat. Some particular examples of these processes are energy production, space cooling, copper material production, heat conduction in tissues, nuclear reactor cooling, and so on. Many researchers have employed baron de Fourier's law [7] of heat conduction, one of the most useful models in continuous mechanics, to improve our understanding of the characteristics of heat transmission. This law has the drawback of producing a parabolic energy equation, which shows how the initial disturbance quickly affects the entire system. Cattaneo [8] used thermal relaxation time to modify traditional Fourier's law in order to control this restriction.By utilizing Oldroyd's upper-convected derivatives to propose a frame-indifferent generalization, Christov [9] enhanced Cattaneo [9]'s approach. In this area, numerous investigations have been conducted since Christov's [9] groundbreaking work. The heat transport model proposed by Cattaneo [8] and Christov [9] for thermal convection in viscous materials was examined by Straughan [10].

The non-Newtonian materials include blood, drilling mud, printer ink, soup, butter, cheese, ketchup, jam, mayonnaise, and hydrogenated colloidal suspension. Powell and Eyring were introduced to the Eyring-Powell fluid model in 1944. The empirical representation of its constitutive link and its Newtonian behavior at both high and low shear rates distinguish this particular model. The sources provide studies that back up the Eyring-Powell fluid model [11–13]. However, a detailed examination of the previously described works reveals that Eyring-Powell is also capable of exhibiting fluid properties that thicken under shear. This explains the discrepancies in the data on the impact of the material characteristic on flow velocity. Analysis of the modified Fourier law for the ferromagnetic flow Zubair et al. [14] investigates the Powell-Eyring fluid with the assumption of two equal magnetic dipoles.

The major objective of this work is to investigate a non-Fourier heat flux on a nonlinear stretched surface in which a two-dimensional Modified Eyring-Powell liquid with double stratified chemical reactive flow is demonstrated. Using a similarity transformation method, the governing expression is transformed into a set of coupled nonlinear ordinary differential systems. Homotopy analysis is used to solve the resulting problems. We examine the temperature, skin friction, and velocity for several of other variables that may be mentioned in the problem statement.

2 Mathematical Modeling

Consider a double stratified chemical reactive flow of non-Fourier heat flux due to a nonlinear stretched surface in a two-dimensional Modified Eyring-Powell liquid. The x-axis is taken along the stretching sheet with the slit at the origin, and the y-axis is normal to the sheet. Thermal conductivity is considered to be temperature-dependent. The Non-Fourier heat flux is utilized in the method of heat transfer. Furthermore, surface is at $y = A(x+b)^{\frac{1-n}{2}}$. We denote the variable concentration at and away from the sheet as (T_∞, C_∞) and the variable temperature as (T_w, C_w). The continuity, momentum and temperature field equations after the boundary approximations are:

$$\partial_x u + \partial_y v = 0, \tag{1}$$

$$u\partial_x u + v\partial_y u = \frac{\mu}{\rho}\partial_{yy} u + \frac{q}{\rho}\left(\frac{1}{BC}\right)^q \left(1 + \frac{q+2}{6C^2}(\partial_y u)^2\right)(\partial_y u)^{q-1}\partial_{yy} u, \tag{2}$$

$$u\partial_x T + v\partial_y T + \lambda^*\big(u\partial_x u\partial_x T + v\partial_y u\partial_y T + v\partial_y u\partial_x T + 2uv\partial_{xy} T + u^2\partial_{xx} T + v^2\partial_{yy} T\big) = -\frac{1}{\rho c_p}k(T)\partial_{yy} T, \tag{3}$$

$$u\partial_x C + v\partial_y C = D\partial_{yy} C - K^*(C - C_\infty), \quad (4)$$

with conditions.

$$\begin{aligned} u &= U_w(x) = U_0(x+b)^n, \\ v &= 0, \\ T &= T_w = T_0 + c(x+b), \end{aligned} \quad (5)$$

$$C = C_w = C_0 + c^*(x+b) \quad \text{at} \quad y = A(x+b)^{\frac{1-n}{2}}, \quad (6)$$

$$\begin{aligned} &u \to 0, \quad T \to T_\infty = T_0 + d(x+b), \\ &C = C_w = C_0 + d^*(x+b) \quad \text{as} \quad y \to \infty. \end{aligned} \quad (7)$$

The thermal conductivity in this case is represented by the formula $k(T) = k_\infty(1+\epsilon_1\theta)$, where k_∞ is the ambient fluid's thermal conductivity, ϵ the small scalar parameter that shows how temperature affects variable thermal conductivity, (b, c, d, c^*, d^*) the dimensionless constants, μ the coefficient of dynamic viscosity, θ the dimensionless temperature, K^* the reaction rate and ρ the fluid density. The fluid parameters in this case are B and C, the Modified Eyring Powell fluid parameters; the specific heat is c_p, T the temperature and T_∞ the ambient temperature, the temperature, and (u, v) are the velocity components in the (x, y) directions, and q is the deformation rate, respectively.

Using the following transformations.

$$\begin{aligned} \chi &= \sqrt{\frac{2}{n+1} U_0 v (x+b)^{n+1}} F(\xi), \\ \xi &= \sqrt{\left(\frac{n+1}{2}\right)\left(\frac{U_0}{v}\right)(x+b)^{n-1}}, \\ u &= U_0(x+b)^n F'(\xi). \end{aligned} \quad (8)$$

$$\begin{aligned} v &= -\sqrt{\left(\frac{n+1}{2}\right) U_0 v (x+b)^{n-1}} \left(F(\xi) + \xi \frac{n-1}{n-1} F'(\xi)\right), \\ \theta(\xi) &= \frac{T - T_\infty}{T_w - T_\infty}, \\ \phi(\xi) &= \frac{C - C}{C_w - C_\infty} \end{aligned} \quad (9)$$

By the use of Eq. (6) into the Eqs.(2-4), we get:

$$\begin{aligned} &(1 + Kq\sqrt{\frac{n+1}{2}\delta F''})^{q-1}(1 - \frac{q+2}{3}\delta(F'')^2)F''' \\ &+ FF'' - \frac{2n}{n+1}(F')^2 = 0. \end{aligned} \quad (10)$$

$$\begin{aligned} &(1+\epsilon_1\theta)\theta'' + \epsilon_1\theta'^2 + PrF\theta' \\ &+ Prr\left(\frac{n-3}{2}F\theta'F' - \frac{n+1}{2}F^2\theta''\right) \\ &+ Pr(S_1+\theta)(rF'F'' - \frac{2}{n+1}F' - \frac{2n}{n+1}rF^2)) = 0. \end{aligned} \quad (11)$$

$$\phi'' + ScF\phi' - \frac{2Sc}{n+1}(S_2F' + \phi F' + \lambda\phi) = 0. \quad (12)$$

with:

$$\begin{aligned} &F'(\alpha) = 1, \quad F(\alpha) = \alpha\frac{1-n}{1+n}, \\ &\theta(\alpha) = 1 - S_1, \quad \phi(\alpha) = 1 - S_2, \\ &F'(\infty) = 0, \quad \theta(\infty) = 0, \quad \phi(\infty) = 0 \end{aligned} \quad (13)$$

Now we have $F(\xi) = f(\xi - \alpha) = f(\eta)$, $\theta(\xi) = \theta(\xi - \alpha) = \theta(\eta)$ and $\phi(\xi) = \phi(\xi - \alpha) = \phi(\eta)$ then Eq. (8-10) becomes.

$$\begin{aligned} &\left(1 + Kq\sqrt{\frac{n+1}{2}\delta f''}\right)^{q-1}\left(1 - \frac{q+2}{3}\delta\left(f''\right)^2\right)f''' \\ &+ ff' - \frac{2n}{n+1}\left(f'\right)^2 = 0. \end{aligned} \quad (14)$$

$$\begin{aligned} &(1+\epsilon_1\theta)\theta'' + \epsilon_1\theta^2 \\ &+ Prf\theta' + Prr\left(\frac{n-3}{2}f\theta'f' - \frac{n+1}{2}f^2\theta''\right) \\ &+ Pr(S_1+\theta)(yff'' - \frac{2}{n+1}f' - \frac{2n}{n+1}yf^2)) = 0. \end{aligned} \quad (15)$$

$$\phi'' + Scf\phi' - \frac{2Sc}{n+1}(S_2F' + \phi F' + \lambda\phi) = 0. \quad (16)$$

with

$$\begin{aligned} &F(0) = 1, \quad F(0) = \alpha\frac{1-n}{1+n}, \\ &\theta(0) = 1 - S_1, \quad \phi(0) = 1 - S_2, \\ &F'(\infty) = 0, \quad \theta(\infty) = 0, \quad \phi(\infty) = 0. \end{aligned} \quad (17)$$

Here $K(=\frac{1}{\mu BC})$ and $\delta(=\frac{U_0^3(x+b)^{3n-1}}{2vC^2})$ are the fluid parameters, The fluid parameters $S_1(=\frac{d}{c})$

and $S_2(=\frac{d^*}{c^*})$, which represent the thermal and solutal stratification parameters, The chemical reaction parameter is represented by $\lambda(=\frac{K^*}{U_0}(x+b)^{1-n})$, Considering that a chemical reaction is considered generative when $\Delta > 0$ and destructive when $\Delta < 0$, $\gamma(=\lambda^* U_0(x+b)^{n-1})$ the thermal relaxation parameter, $Sc(=\frac{v}{D})$ the schmidt number and $Pr(=\frac{v}{a})$.

The skin friction coefficient and sherwood number can be expressed as:

$$C_f = \frac{2\tau_w}{\rho U_w^2}, \quad Sh_x = \frac{(x+b)q_m}{D(C_w - C_0)}. \tag{18}$$

where

$$\begin{aligned} \tau_w &= \mu\partial_y u + \frac{1}{BC}\partial_y u - \frac{1}{6BC^3}(\partial_y u)^3 \\ \text{and } q_w &= D\partial_y C \text{ at } y = A(x+b)^{\frac{1-n}{2}}. \end{aligned} \tag{19}$$

The dimensionless form is:

$$\begin{aligned} \frac{\sqrt{Re_x}C_f}{2} &= \sqrt{\frac{n+1}{2}\left(1 + K - \frac{n+1}{2}\frac{K\delta}{3}f'(0)\right)}f'(0) \\ \text{and } \sqrt{Re_x}Sh_x &= \sqrt{\frac{n+1}{2}}\phi'(0), \end{aligned} \tag{20}$$

where $Re_x = \frac{u_w(x+b)}{v}$ the local Reynolds number.

3 Homotopic Procedure

The convergent solutions of Eqs. (11-13) have been obtained through the use of the HAM approach, with the boundary conditions in Eq. (14). Series form is consistent with the solutions. The first approximations and operators are written as follows:

$$\begin{aligned} f_0(\eta) &= 1 - e^{-\eta}, \\ \theta_0(\eta) &= (1 - S_1)e^{-\eta}, \\ \phi_0(\eta) &= (1 - S_2)e^{-\eta}, \end{aligned} \tag{21}$$

$$L_f = f'' - f', \quad L_\theta = \theta'' - \theta', \quad L_\phi = \phi'' - \phi'. \tag{22}$$

with

$$\begin{aligned} L_f[C_1 + C_2e^{\eta} + C_3e^{-\eta}] &= 0, \\ L_\theta[C_4e^{\eta} + C_5e^{-\eta}] &= 0, \\ L_\phi[C_6e^{\eta} + C_7e^{-\eta}] &= 0. \end{aligned} \tag{23}$$

where $C_i(i = 1-7)$ defines the arbitrary constants.

4 Homotopic Procedure

H-Curve plays a very important role in the HAM approach, it basically shows the convergence region for Eq.(10) and Eq.(11) with the use of Eq.(12). It is observed that suitable values are: $-1.0 \le h_f \le -0.5$, $-1.0 \le h_\theta \le -0.3$ and $-1.2 \le h_\phi \le -0.4$. The H-Curve is displayed in Figure 1.

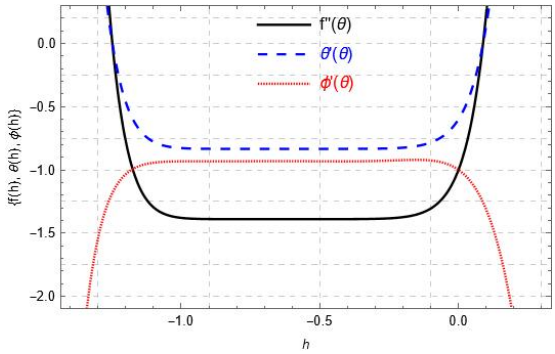

Figure 1. H-Curve for f'', θ and ϕ.

5 Stability Analysis

The stability analysis for the solutions is pictured in the following Figure 2 when $n = \delta = S_1 = 0.6, K = \epsilon_1 = \lambda = q = 0.4, S_2 = \gamma = \alpha = 0.1, Sc = 0.8$ and $Pr = 0.9$. The graphic illustrates how the velocity gradient stabilizes at recursive step 20 and stays that way. On the other hand, the temperature gradient and concentration stabilizes at recursive step 30 and elsewhere.

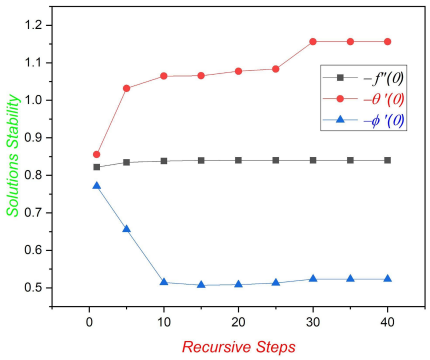

Figure 2. Stability Analysis.

6 Analysis

The outcomes of key variables on skin friction, temperature, and velocity are addressed in this section. To achieve this, Figures 3 to 17 are presented.

The behavior of K on f' is shown in Figure 3. It is investigated whether f' and the layer thickness

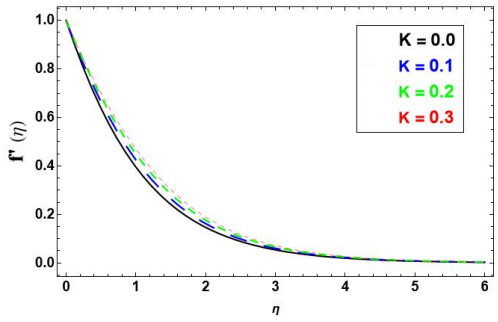

Figure 3. K via f'.

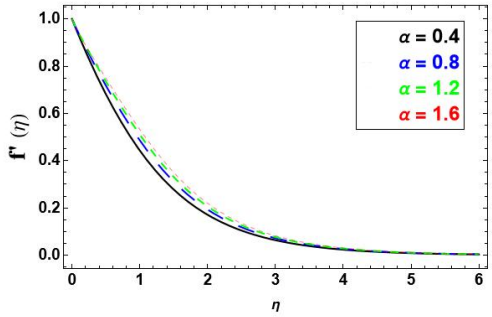

Figure 4. α via f'.

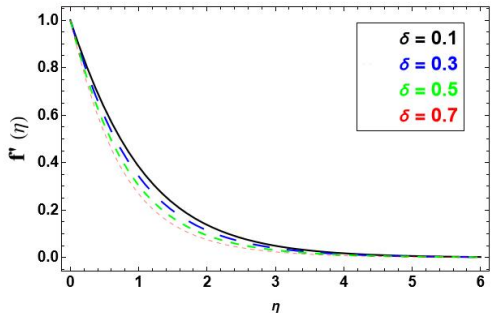

Figure 5. δ via f'.

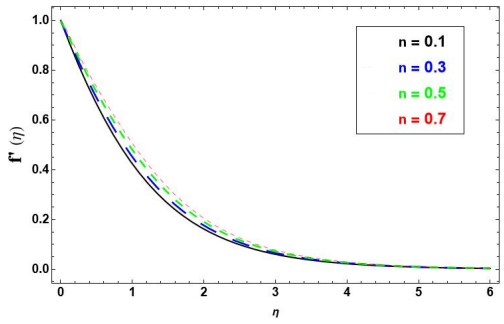

Figure 6. n via f'.

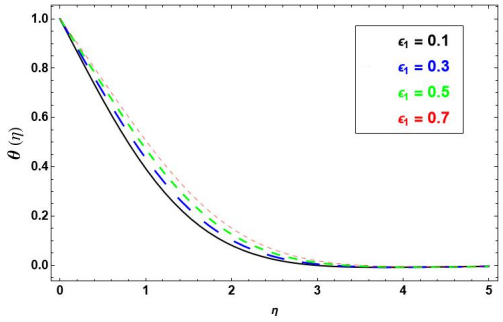

Figure 7. ε_1 via f'.

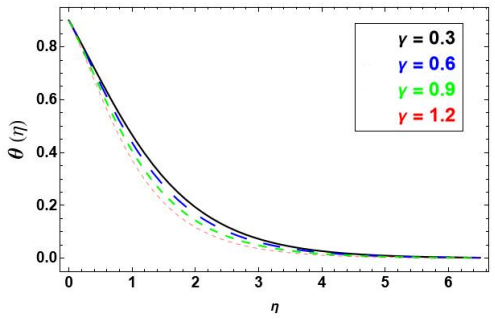

Figure 8. γ via f'.

that corresponds to it improves. Increased velocity and momentum layer thickness, as well as decreased viscosity, are the effects of higher K. Figure 4 illustrates how α affects f'. The velocity and momentum layer thickness grow with increasing α. Figure 5 displays the characteristics of δ on f'. Here, the velocity and associated layer thickness show decreasing behavior for larger δ. The behavior of n on velocity f' is depicted in Figure 6. It is evident that as n increases, so does f'. Figure 7 shows the impact of ϵ_1 on temperature θ. A larger ϵ_1 increases the temperature θ. In terms of physical properties, thermal conductivity increases with bigger ϵ_1 because it allows for significant heat transfer from the sheet to the substance, which raises temperature θ. The behavior of γ on temperature θ is seen in Figure 8. Here, the function of γ is decreasing with temperature θ. In addition, heat transport occurs quickly when $\gamma = 0$. The behavior of S_1 at temperature θ is displayed in Figure 9. In this case, as S_1 is enhanced, temperature θ and thermal layer thickness decrease. For larger S_1, the physical difference between the ambient and surface temperature θ decreases. It is corresponding to a decrease in temperature θ. The behavior of n at temperature θ is depicted in Figure 10. It is evident that temperature θ rises as n increases. Figure 11 shows the effect of Pr on temperature θ. An increase in Pr will result in a large decrease in the thermal boundary layer and temperature θ.

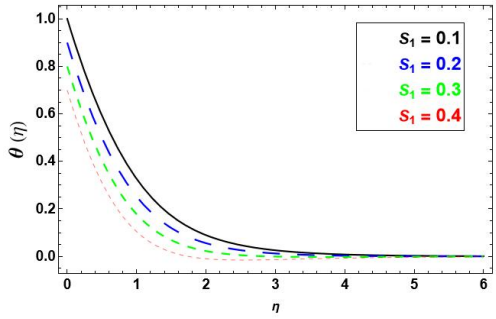

Figure 9. S_1 via θ.

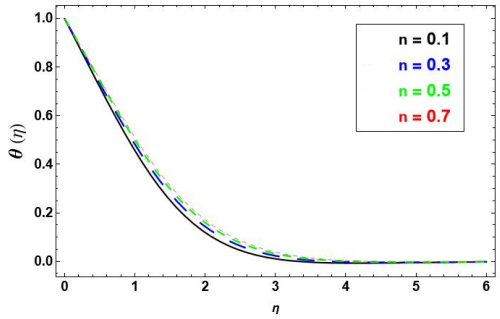

Figure 10. n via θ.

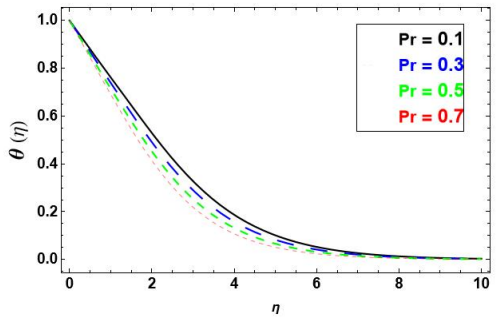

Figure 11. S_2 via ϕ.

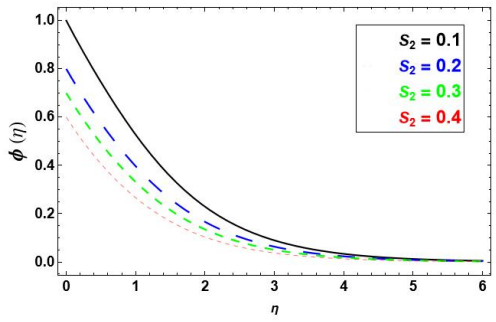

Figure 12. S_2 via ϕ.

Figure 12 discusses the function of S_2 on Concentrations ϕ. Take note that Concentrations ϕ decreases as S_2 increases. The reason for this is that as S_2 increases, the difference between the ambient and surface concentrations ϕ decreases, causing concentrations ϕ to decay. The properties of Sc on concentrations ϕ are displayed in Figure 13. For larger Sc, concentrations ϕ here decrease. Actually, there is a lesser Brownian diffusion coefficient for bigger Sc, which has caused concentrations ϕ decreases. The effect that λ has on concentrations ϕ is shown in Figure 14. As λ is increased in this case, concentrations ϕ and the thickness of the corresponding layer decreases. Furthermore, when $\lambda > 0$ is compared to $\lambda < 0$, it is seen that the behavior is quite opposite. The behavior of n on concentrations ϕ is depicted in Figure 15. It is evident that temperature θ rises as n increases. Figure 16 displays the characteristics of K and δ on skin friction. Higher K causes skin friction to rise whereas greater δ causes it to decrease. The behaviors of Sc and λ on Sherwood number are discussed in Figure 17. There is no doubt that Sherwood's number rises as Sc and λ increase. Table 1 demonstrates the convergence of the series solutions. It is evident that, for temperature, concentration, and velocity, respectively, the convergence starts at the 30th order of approximations. The stability analysis for the solutions is depicted in the Figure 2.

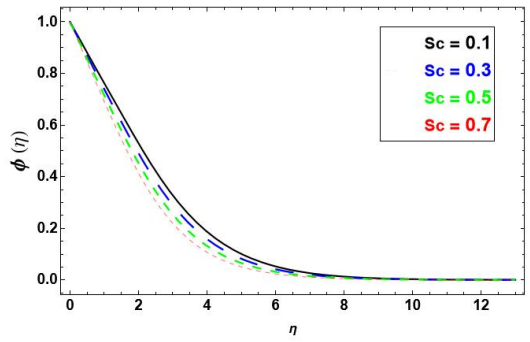

Figure 13. Sc via ϕ.

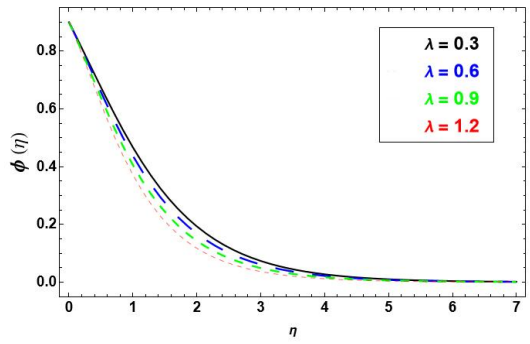

Figure 14. λ via ϕ.

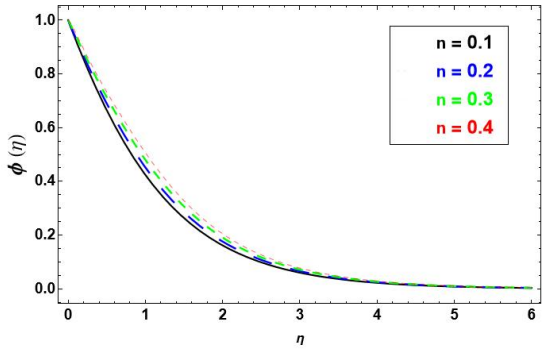

Figure 15. n via ϕ.

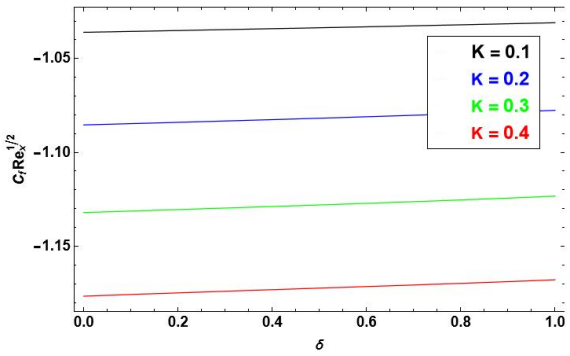

Figure 16. Skin Friction on K anf δ.

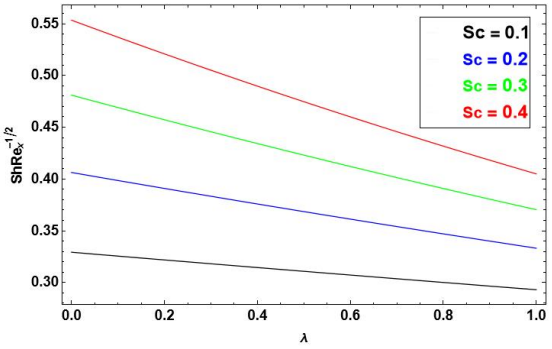

Figure 17. Sherwood on Sc via λ.

7 Conclusions

The following important points are included in the summary of this article's conclusion:

- For increasing n, there is an increase in temperature θ, concentration ϕ, and velocity f'.
- As K increases, the viscosity decreases, increasing the thickness of the momentum and velocity layers.
- Non-Fourier's heat flux has a temperature that is lower than Fourier's approach.
- Greater α results in increased velocity and thickness of the momentum layer.

Table 1. The Homotopic solutions for convergence when $n = \delta = S_1 = 0.6, K = \epsilon_1 = \lambda = q = 0.4, S_2 = \gamma = \alpha = 0.1, Sc = 0.8$ and $Pr = 0.9$.

Approximation Order	$-f''(0)$	$-\theta'(0)$	$-\phi'(0)$
1	0.8219	0.8554	0.7712
5	0.8346	1.0318	0.6555
10	0.8381	1.0646	0.5145
15	0.8394	1.0655	0.5073
20	0.8401	1.0775	0.5087
25	0.8401	1.0835	0.5129
30	0.8401	1.1563	0.5236
35	0.8401	1.1563	0.5236
40	0.8401	1.1563	0.5236

- When ϵ_1 increases, temperature decreases when Pr and χ increase.
- Temperature θ and concentrations ϕ decreases as S_1 and S_2 increases.

Data Availability Statement

Data will be made available on request.

Funding

This work was supported without any funding.

Conflicts of Interest

The authors declare no conflicts of interest.

Ethical Approval and Consent to Participate

Not applicable.

References

[1] Srinivas, S., Malathy, T., & Reddy, A. S. (2016). A note on thermal-diffusion and chemical reaction effects on MHD pulsating flow in a porous channel with slip and convective boundary conditions. *Journal of King Saud University-Engineering Sciences, 28*(2), 213-221. [CrossRef]

[2] Zhang, C., Zheng, L., Zhang, X., & Chen, G. (2015). MHD flow and radiation heat transfer of nanofluids in porous media with variable surface heat flux and chemical reaction. *Applied Mathematical Modelling, 39*(1), 165–181. [CrossRef]

[3] Mabood, F., Khan, W. A., & Ismail, A. I. M. (2015). MHD stagnation point flow and heat transfer impinging on a stretching sheet with chemical reaction and transpiration. *Chemical Engineering Journal, 273*, 430–437. [CrossRef]

[4] Mythili, D., & Sivaraj, R. (2016). Influence of higher order chemical reaction and nonuniform heat source/sink on Casson fluid flow over a vertical cone and flat plate. *Journal of Molecular Liquids, 216*, 466–475. [CrossRef]

[5] Eid, M. R. (2016). Chemical reaction effect on MHD boundary-layer flow of two-phase nanofluid model over an exponentially stretching sheet with a heat generation. *Journal of Molecular Liquids, 220*, 718–725. [CrossRef]

[6] Makinde, O. D., & Animasaun, I. L. (2016). Thermophoresis and Brownian motion effects on MHD bioconvection of nanofluid with nonlinear thermal radiation and quartic chemical reaction past an upper horizontal surface of a paraboloid of revolution. *Journal of Molecular Liquids, 221*, 733–743. [CrossRef]

[7] baron de Fourier, J. B. J. (1822). *Théorie analytique de la chaleur*. Firmin Didot.

[8] Cattaneo, C. (1948). Sulla conduzione del calore. *Atti del Seminario Matematico e Fisico dell'Università di Modena e Reggio Emilia, 3*, 83–101.

[9] Christov, C. I. (2009). On frame indifferent formulation of the Maxwell-Cattaneo model of finite-speed heat conduction. *Mechanics Research Communications, 36*(4), 481–486. [CrossRef]

[10] Straughan, B. (2010). Thermal convection with the Cattaneo–Christov model. *International Journal of Heat and Mass Transfer, 53*(1–3), 95–98. [CrossRef]

[11] Hayat, T., Waqas, M., Shehzad, S. A., & Alsaedi, A. (2017). Mixed convection stagnation-point flow of Powell-Eyring fluid with Newtonian heating, thermal radiation, and heat generation/absorption. *Journal of Aerospace Engineering, 30*(1), 04016077. [CrossRef]

[12] Hayat, T., Zubair, M., Ayub, M., Waqas, M., & Alsaedi, A. (2016). Stagnation point flow towards nonlinear stretching surface with Cattaneo-Christov heat flux. *The European Physical Journal Plus, 131*(10), 355. [CrossRef]

[13] Hayat, T., Zubair, M., Waqas, M., Alsaedi, A., & Ayub, M. (2017). On doubly stratified chemically reactive flow of Powell–Eyring liquid subject to non-Fourier heat flux theory. *Results in Physics, 7*, 99-106. [CrossRef]

[14] Zubair, M., Ijaz, M., Abbas, T., & Riaz, A. (2019). Analysis of modified Fourier law in flow of ferromagnetic Powell–Eyring fluid considering two equal magnetic dipoles. *Canadian Journal of Physics, 97*(7), 772–776. [CrossRef]

Dr. Muhammad Zubair is working as a postdoc fellow in the School of Qilu Transportation, Shandong University, Jinan, 250061, China. He is working mainly in the field of Newtonian and non-Newtonian computational fluid dynamics, porous media, heat and mass transfer, stretching sheets, stretching cylinders, applied mathematics, exact solutions, artificial intelligence, discrete element methods, etc. (Email: mzubair@sdu.edu.cn)